

can only be achieved at the cost of considerable emitting power levels. In most environments the signal will illuminate the receiver from privileged directions coinciding frequently with the direction of the emitter. The noise can be separated into internal and external components: the receiver noise, produced by the front-end electronics, and the ambient noise, produced by artificial and natural light sources. The receiver noise is obviously isotropic. However, in most environments the ambient noise is dominant over the receiver noise. The ambient noise emanates from particular directions coinciding frequently with the positions of the lamps (fluorescent and/or incandescent artificial light) and of the windows (sun light) of a room. Moreover, in contrast with the signal sources, the ambient light noise sources are usually in line-of-sight with the receiver. Also recent trends in indoor illumination point out to the widespread use of spot lights. This document proposes and studies a novel receiver structure for indoor optical wireless communication systems that exploits the directional nature in both signal and noise propagation through the use diversity techniques. To the best knowledge of the authors it is the first time that the use of diversity principles is proposed and studied in this context. In this document we concentrate on the ability of the proposed sectored receiver in combating the ambient noise. However, a sectored receiver is also very effective in combating both multipath dispersion and co-channel interference. This will be the subject of future contributions.

The proposed receiver is formed by multiple sectors (also called diversity branches) and operates by choosing the sector with the best signal-to-noise ratio (SNR) or some desirable additive combination of the total signals of all sectors. Each sector comprises an optical collector with a particular active area, orientation and field-of-view plus its associated front-end and control circuits. Each sector sees only a portion of the overall field-of-view in such a way that the set of all sectors will cover the entire field-of-view. An additional advantage of using a narrower field-of-view is that lenses can be used as optical collectors which allows the increase of the receiver active area at low cost.

We will consider both diffuse and quasi-diffuse systems. In a diffuse system the emitted signal fills the whole volume of the room through multiple reflections in its walls and obstacles. In this way the collected signal is independent of the position and orientation of the receiver. A quasi-diffuse system makes use of only one reflection surface which is usually the ceiling of the room. In contrast with radio systems this is possible in optical wireless systems since typical ceiling surfaces present good scattering and reflection properties to the optical radiation. Diffuse systems are more appropriate for mobile terminals while quasi-diffuse systems are more appropriate for fixed (e.g. desktop) terminals.

Diversity techniques have been used extensively in radio systems to combat the effects of signal fading [4, 1]. The diversity technique here proposed is conceptually close to angle diversity which has been suggested for tropospheric scatter systems [5].

In this document we will compare the performances of sectored and non-sectored receivers under several conditions. In sections II and III we present the signal propagation model and the ambient noise model, respectively. In section IV we present the combining methods under study. In section V we define the diversity gain. In section VI we present and discuss the results. In section VII we discuss some implementation issues. Finally, in section VIII we present our conclusions.

This work is being carried out as part of the ESPRIT.6892 POWER (Portable Workstation for Education in Europe) project commissioned by the CEC.

II. Signal Propagation Model

The signal propagation model includes the emitter radiation pattern, the channel propagation characteristics and the receiver collecting pattern.

A. Emitter Model

The optical emitter is modelled as a generalised Lambertian source. The radiant intensity in a direction at an angle θ from the normal to the emitting surface is given by:

$$I(\theta) = P_E \frac{n+1}{2\pi} \cos^n \theta \quad (2.1)$$

where:

$$n = \frac{\ln(1/2)}{\ln(\cos hpa)} \quad (2.2)$$

P_E is the total emitted power and hpa is the half-power angle of the emitter. The orientation of the emitter is defined by the elevation and azimuth angles ($\theta_{E_d}, \varphi_{E_d}$). The position of the emitter is defined by its coordinates relative to the cell centre ($x_E, y_E, z_E=0$). In figure 2.1 we represent the radiant intensity profile of an emitter with $hpa=40^\circ$, $\theta_{E_d}=45^\circ$ and $\varphi_{E_d}=45^\circ$.

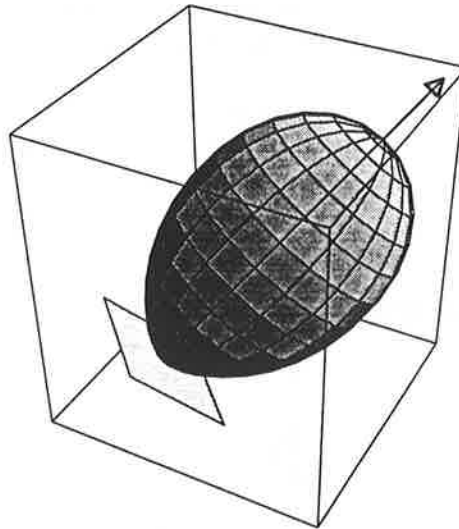


Figure 2.1: Radiant intensity profile of a generalised Lambertian emitter with $hpa = 40^\circ$, $\theta_{E_d} = 45^\circ$ and $\varphi_{E_d} = 45^\circ$.

B. Sectorized Receiver Model

The sectorized receiver is assumed to be a hemisphere where a set of parallels and equally spaced meridians define the boundaries of the sectors. We will refer to the

region of the sectored receiver enclosed between two parallels as a *segment*. The sectored receiver can be completely specified through a set Ψ with a subset for each segment indicating the number of sectors, the azimuth offset of the first sector and the limiting elevation angles in that segment. We note that all sectors belonging to the same segment have an equal azimuth span. An example of a sectored receiver is represented in figure 2.2.

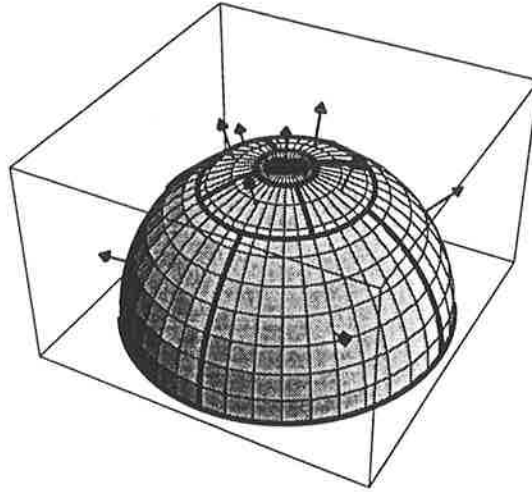


Figure 2.2: Sectored receiver with 3 segments: $\Psi = \{ \{1, 0^\circ, 0^\circ, 10^\circ\}, \{4, 45^\circ, 10^\circ, 30^\circ\}, \{4, 0^\circ, 30^\circ, 90^\circ\} \}$.

The field-of-view of a sector is completely specified by the two limiting elevation angles, θ_h and θ_l , and the two limiting azimuth angles, φ_h and φ_l , where $\theta_h \geq \theta_l$ and $\varphi_h \geq \varphi_l$. We will refer to this model as the pie-shaped field-of-view model. The model imposes no constraints on the active area assigned to each sector. Here we consider the active area of a sector proportional to the sector area and normalised for a unitary area hemisphere. Thus, the active area of a sector is given by:

$$A_{R_s} = \frac{(\varphi_h - \varphi_l)}{2\pi} (\cos \theta_l - \cos \theta_h) \quad (2.3)$$

The orientation of each sector is defined as:

$$\begin{aligned} \theta_{R_s} &= \frac{\theta_h + \theta_l}{2} \\ \varphi_{R_s} &= \frac{\varphi_h + \varphi_l}{2} \end{aligned} \quad (2.4)$$

except in the case of a polar segment with a single sector (θ_h any, $\theta_l=0$, $\varphi_h - \varphi_l=2\pi$) where $\theta_{R_s}=0$ (see figure 2.2). The position of the sectored receiver is defined by its coordinates relative to the cell centre ($x_R, y_R, z_R=0$).

The field-of-view of an optical collector is more commonly modelled as a cone-shaped aperture [2, 3]. In this case the optical collector would see elliptical zones at the reflecting surface. In the case of a sectored receiver these zones will necessarily overlap. The pie-shaped field-of-view model here adopted assures that there is no overlap between the zones seen by each sector. This will be of importance since it will allow studies to be carried out independently of the overlapping factor. In figure

2.3 we show the sectored receiver of figure 2.2 and represent its field-of-view profile, highlighted in one of the sectors, and the ceiling zones seen by each sector.

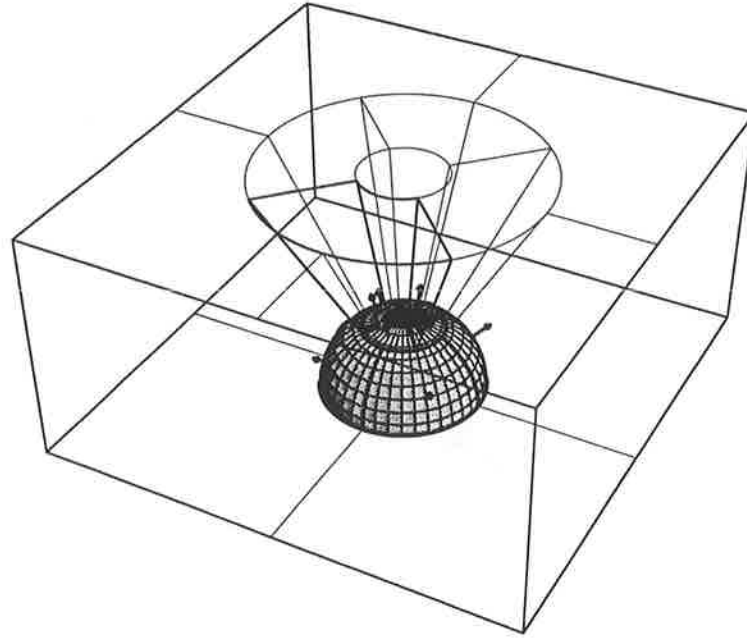


Figure 2.3: Sectored receiver with representation of field-of-view profile and ceiling zones seen by each sector.

C. Diffuse Optical Channel

Following [2] the signal power received in a sector from a diffusely reflecting surface is given by:

$$P_{dif_s} = \frac{w}{2\pi} A_{R_s} \left[\cos \theta_{R_s} (\varphi_h - \varphi_l) (\sin^2 \theta_h - \sin^2 \theta_l) \right. \\ \left. + \sin \theta_{R_s} (\theta_h - \theta_l + \sin \theta_l \cos \theta_l - \sin \theta_h \cos \theta_h) (\sin(\varphi_h - \varphi_{R_s}) - \sin(\varphi_l - \varphi_{R_s})) \right] \quad (2.5)$$

where w is the signal power emitted per surface area into the hemisphere, assumed constant over the reflecting surface, and A_{R_s} is the active area of the sector. The received power is independent of the position of the sectored receiver but depends on the orientation of each sector. In the case of a single sector conical field-of-view receiver ($\theta_h = \pi/2$, $\theta_l = 0$, $\varphi_h - \varphi_l = 2\pi$, $\theta_{R_s} = 0$) the previous expression reduces to that presented in [2].

D. Quasi-Diffuse Optical Channel

A quasi-diffuse channel uses a single reflection surface. The following assumptions are considered: the reflecting surface is an infinite plane; the emitter and receiver move on a plane parallel to the reflecting surface; the reflection coefficient ρ is constant over the reflecting surface. The reference model is represented in figure

2.4. Under these assumptions, the optical power density at the receiver with active area A_R , expressed in terms of receiver cylindrical coordinates $(\rho_R, \varphi_R, z_R = h)$, is given by:

$$dP_R(\rho_R, \varphi_R) = \frac{n+1}{2\pi^2} P_E \rho \frac{A_R}{h^2} \cos^3 \theta_E \cos^n \beta_E \cos \beta_R \frac{\rho_R h}{(h^2 + \rho_R^2)^{3/2}} d\rho_R d\varphi_R \quad (2.6)$$

where, using solid angle geometry:

$$\cos \beta_E = \cos \theta_{E_d} \cos \theta_E + \sin \theta_{E_d} \sin \theta_E (\cos \varphi_{E_d} \cos \varphi_E - \sin \varphi_{E_d} \sin \varphi_E) \quad (2.6.a)$$

$$\cos \theta_E = \frac{h}{\sqrt{\rho_R^2 + h^2 + R_p^2 + 2\rho_R R_p \cos(\varphi_p - \varphi_R)}} \quad (2.6.b)$$

$$\sin \theta_E = \sqrt{1 - \cos^2 \theta_E} \quad (2.6.c)$$

$$\cos \varphi_E = \frac{\rho_R \cos \varphi_R + R_p \cos \varphi_p}{\sqrt{\rho_R^2 + R_p^2 + 2\rho_R R_p \cos(\varphi_p - \varphi_R)}} \quad (2.6.d)$$

$$\sin \varphi_E = \frac{\rho_R \sin \varphi_R + R_p \sin \varphi_p}{\sqrt{\rho_R^2 + R_p^2 + 2\rho_R R_p \cos(\varphi_p - \varphi_R)}} \quad (2.6.e)$$

$$\cos \beta_R = \cos \theta_{R_s} \frac{h}{\sqrt{h^2 + \rho_R^2}} + \sin \theta_{R_s} \frac{\rho_R}{\sqrt{h^2 + \rho_R^2}} \cos(\varphi_{R_s} - \varphi_R) \quad (2.6.f)$$

The coordinates (R_p, φ_p) determine the receiver position relative to the emitter coordinate axis. In terms of cell centre coordinates it results:

$$R_p = \sqrt{(x_R - x_E)^2 + (y_R - y_E)^2} \quad (2.7.a)$$

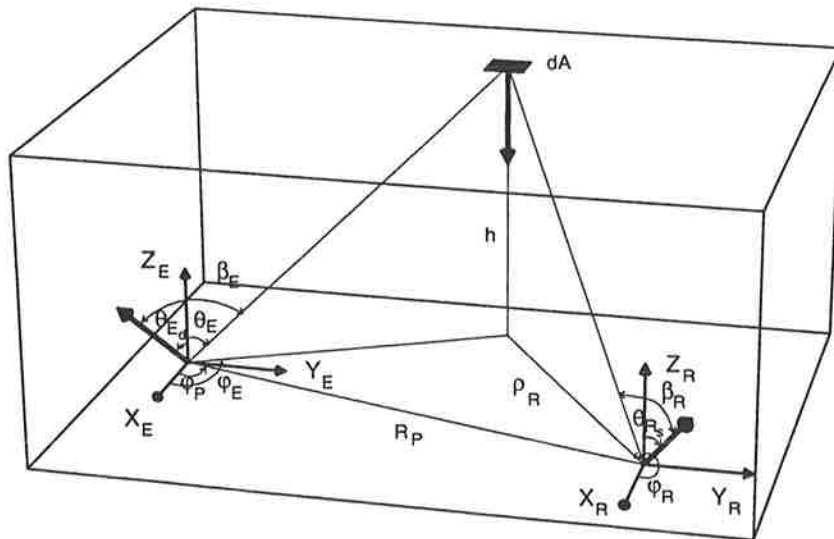


Figure 2.4: Reference model of quasi-diffuse channel.

$$\varphi_p = \arctan\left(\frac{y_R - y_E}{x_R - x_E}\right) \quad (2.7.b)$$

In case the emitter is oriented vertically ($\theta_{E_d}=0$) the optical power density at the receiver reduces to:

$$dP_R(\rho_R, \varphi_R) = \frac{n+1}{2\pi^2} P_E \rho \frac{A_R}{h^2} \cos^{n+3} \theta_E \cos \beta_R \frac{\rho_R h}{(h^2 + \rho_R^2)^{3/2}} d\rho_R d\varphi_R \quad (2.8)$$

Finally, the power collected at the receiver is given by:

$$P_R = \int_{\varphi_l \rho_l}^{\varphi_h \rho_h} dP_R(\rho_R, \varphi_R) \quad (2.9)$$

where $\rho_l = h \tan \theta_l$ and $\rho_h = h \tan \theta_h$.

III. Ambient Noise Model

The system design is usually determined by the ambient noise level since in typical environments this is dominant over the receiver noise. We will define an ambient noise model based on two components: isotropic and directional noise. The isotropic noise is assumed to be collected from a diffusely reflecting surface and is independent of the position of the receiver. Therefore equation (2.5) still applies and the isotropic noise is given by:

$$N_{dif_i} = \frac{w_n}{2\pi} A_{R_i} \left[\cos \theta_{R_i} (\varphi_h - \varphi_l) (\sin^2 \theta_h - \sin^2 \theta_l) + \sin \theta_{R_i} (\theta_h - \theta_l + \sin \theta_l \cos \theta_l - \sin \theta_h \cos \theta_h) (\sin(\varphi_h - \varphi_{R_i}) - \sin(\varphi_l - \varphi_{R_i})) \right] \quad (3.1)$$

where now w_n is the noise power emitted per surface area into the hemisphere.

The directional noise sources are modelled with a generalised Lambertian radiation pattern and assumed to be positioned at the ceiling and oriented vertically. A directional noise source is then completely specified in terms of its total power P_n , its half-power angle hpa_n and its position at the ceiling relative to the cell centre ($x_N, y_N, z_N=h$). Because of the underlying field-of-view model a directional noise source is only seen by one sector. A directional noise source seen at the boundary of a set of sectors is assigned to the sector that sees higher elevation and azimuth angles. The directional noise power contribution from a given noise source is then:

$$N_{dir_i} = \frac{n_n+1}{2\pi} P_n \cos^{n_n+2} \theta_{R_n} \frac{A_{R_i}}{h^2} \cos \beta_{R_n} \quad (3.2)$$

where:

$$\cos \beta_{R_n} = \cos \theta_{R_i} \cos \theta_{R_n} + \sin \theta_{R_i} \sin \theta_{R_n} \cos(\varphi_{R_i} - \varphi_{R_n}) \quad (3.2.a)$$

($\theta_{R_n}, \varphi_{R_n}$) define the position of the noise source in the receiver coordinate axis and:

$$\cos \theta_{R_n} = \frac{h}{\sqrt{(x_N - x_R)^2 + (y_N - y_R)^2 + h^2}} \quad (3.2.b)$$

$$\sin \theta_{R_n} = \sqrt{1 - \cos^2 \theta_R} \quad (3.2.c)$$

$$\cos \varphi_{R_n} = \frac{x_N - x_R}{\sqrt{(x_N - x_R)^2 + (y_N - y_R)^2}} \quad (3.2.d)$$

$$\sin \varphi_{R_n} = \frac{y_N - y_R}{\sqrt{(x_N - x_R)^2 + (y_N - y_R)^2}} \quad (3.2.e)$$

The relation between isotropic and directional noise is controlled by the noise ratio parameter, NR , which is the ratio of the directional noise power to the isotropic noise power collected at the cell centre by the sectored receiver. We note that the receiver noise is also accommodated in this model through its isotropic noise component. In order to allow meaningful comparisons whenever the noise ratio is varied the total noise seen by the sectored receiver at the cell centre is kept constant by adjusting both the isotropic and directional noise levels.

Without loss of generality, the ambient light is assumed to be stationary. The signal dependent shot noise is also assumed negligible. The stationary ambient light produces shot noise upon impinging on the photodetector. The shot noise arises from the statistical nature of the production of photocarriers. It has a mean square value in a bandwidth B which is proportional to the average value of the photocurrent I_p :

$$\sigma^2 = 2qBI_p \quad (3.3)$$

Throughout this study we assume a constant bandwidth and normalise the factor $2qB$ to unity.

IV. Combining methods

We will consider two types of linear combining methods: maximal-ratio and selection combining [4].

In a selection combining receiver only the sector with the best SNR is chosen. We will also refer to the receiver operating under this method as the best-sector receiver. Lets denote the average signal and rms noise referred to the input in sector j by i_j and σ_j respectively. Assuming N sectors, the output SNR of the selection receiver is given by:

$$\left(\frac{i}{\sigma}\right)_s = \max_j \left[\frac{i_j}{\sqrt{\sigma_j^2}} \right] \quad (4.1)$$

Under the assumption of independent noise, the optimum output SNR is achieved by the maximal-ratio combining receiver. In this receiver the total signals from each sector are weighted by a gain proportional to the ratio i/σ^2 of the sector and then added together. The SNR of a maximal-ratio combining receiver is given by [4]:

$$\left(\frac{i}{\sigma}\right)_{MR} = \sqrt{\sum_{j=1}^N \left(\frac{i_j}{\sigma_j}\right)^2} \quad (4.2)$$

Clearly the advantages of the combining methods are best achieved as the unbalancing in the distribution of the SNR among the sectors increases.

We normalise the responsivity of the photodiode to unity. Therefore, in a given sector, $i = P_R$ and $\sigma^2 = N_{dir} + N_{iso}$.

V. Diversity gain

In practice optical wireless systems are usually designed for a worst-case SNR. The SNR is a function of the characteristics and relative position of emitter, receiver, reflecting surfaces and directional noise sources and of the relative strength of isotropic noise and directional noise. We define the *diversity gain* or *diversity improvement* as the ratio of the worst-case SNR of the sectored receiver to the worst-case SNR of a non-sectored reference receiver. The reference receiver is considered to be vertically oriented and with a field-of-view of 90° (a single sector receiver with $\theta_h = \pi/2$, $\theta_l = 0$, $\varphi_h - \varphi_l = 2\pi$). This is the preferred configuration for non-sectored receivers in quasi-diffuse and diffuse systems. For normalisation purposes we will also consider the active area of the non-sectored receiver equal to the sum of the active areas of all sectors of the sectored receiver.

VI. Discussion and Results

We will consider the default configuration represented in figure 6.1 with the following characteristics: i) the sectored receiver has 8 sectors on a single segment with a null offset on the azimuth of the first sector: $\Psi = \{8, 0^\circ, 0^\circ, 90^\circ\}$; ii) there are 4 directional noise sources positioned at the reflecting surface at azimuth directions 45° , 135° , 225° and 315° and distance to the ceiling centre $r_n = p_n \sqrt{2} = 3\sqrt{2}$; the half power angle of the noise sources is $hpa_n = 25^\circ$; the total power emitted by the directional noise sources P_n is unity; all directional noise sources emit the same total

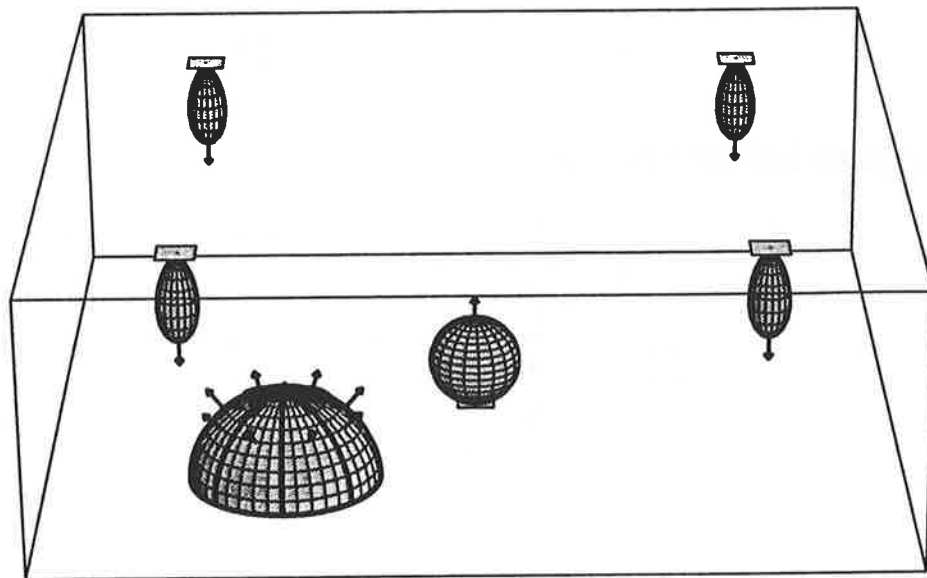


Figure 6.1: Default room configuration model.

power; iii) the emitter has an half power angle of $hpa=60^\circ$ and is positioned at the cell centre; the total emitted power P_E is unity; iv) the cell is rectangular with a 12 x 12 meters range; the height of the ceiling is $h=3$ meters; the reflection coefficient of the ceiling surface ρ is unity; v) the noise ratio value is $NR=10$; vi) the level of isotropic noise can be calculated at the cell centre from the default values of the noise ratio parameter and of the total power emitted by the directional noise sources. In this section we will carry out several studies by varying some of the parameters of this default configuration.

In the default configuration a sectored receiver positioned at the cell centre will have 4 sectors illuminated with both isotropic and directional noise (at equal levels) while the other 4 sectors will be only illuminated by isotropic noise (also at equal levels). In order to elucidate the meaning of the noise ratio parameter we relate it in figure 6.2 with the percentage of directional noise seen by one of the mixed noise sectors. For noise ratios of 0.1, 0.5 and 10 the percentages are 16.7%, 50% and 95.2%.

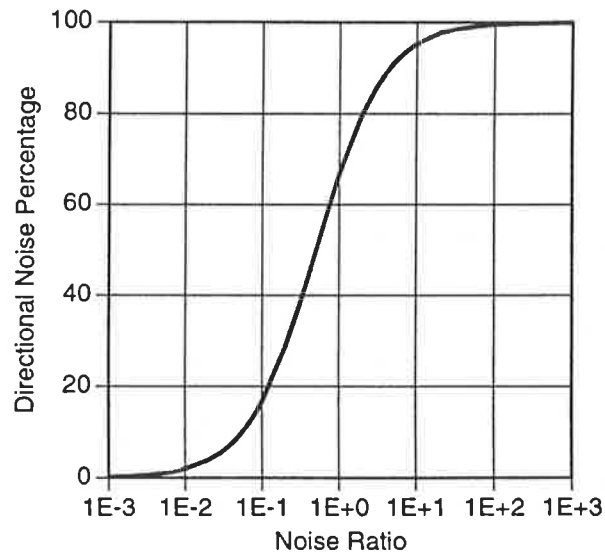
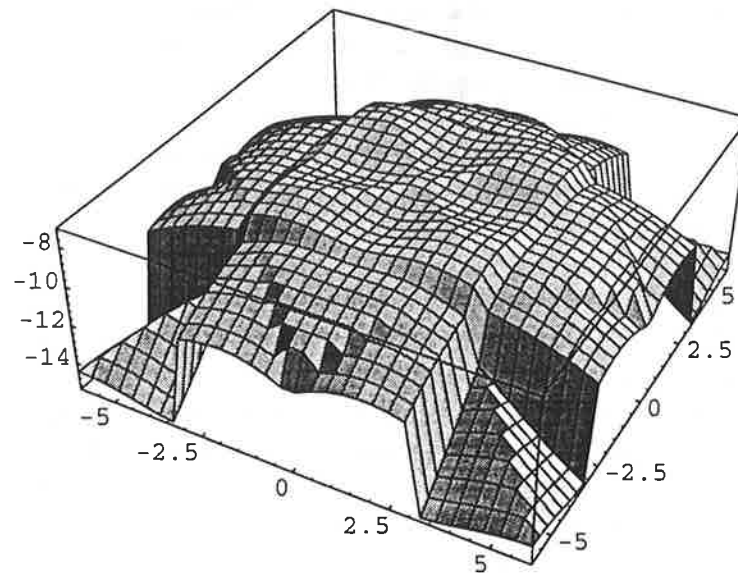


Figure 6.2: Percentage of directional noise seen by one mixed noise sector as a function of the noise ratio parameter.

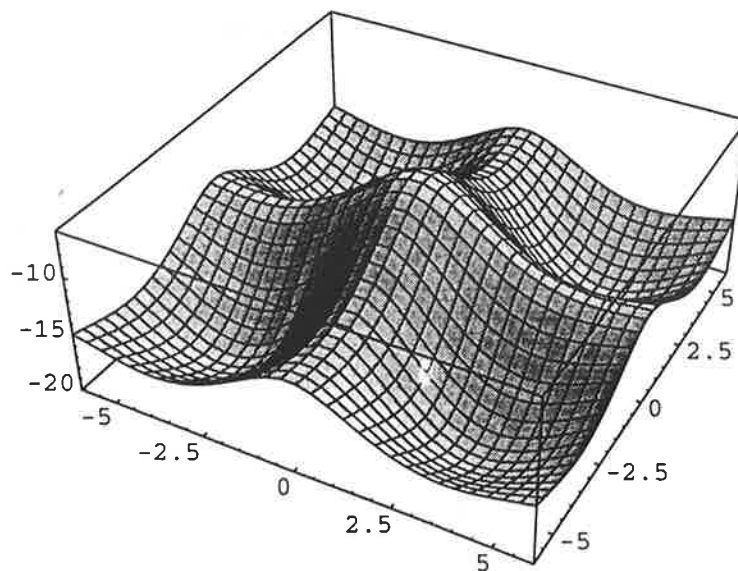
A. Quasi-Diffuse systems

Figure 6.3 shows the SNR of the maximal-ratio sectored and non-sectored receivers as a function of position within the default configuration room. As seen in figure 6.3.b the SNR of the non-sectored receiver has its maximum at the cell centre and shows a saddle zone below the noise sources, corresponding to an increase in the intensity of the directional noise. We note that in the case of the non-sectored receiver the signal has a maximum at the cell centre while the noise has a maximum below the noise sources. The SNR of the sectored receiver (figure 6.3.a) maintains a relatively constant level but drops significantly at positions of the sectored receiver where most of the signal and directional noise power are collected from the same direction, i.e., zones where the closest directional noise source is interposed between the emitter and the receiver. This effect suggests that the diversity gain will be higher

in system configurations where one or several directional noise sources are positioned outside the cell. An obvious common case is a room with windows. This effect also suggests that the diversity gain will be higher in a multicell environment where co-channel interference dominates the system design. As defined in section V, the diversity gain is computed from the difference between the worst-case SNR of the sectored and non-sectored receivers corresponding to the difference between the global minima of the SNR surfaces shown in figure 6.3. In the default configuration the diversity gain of the maximal-ratio receiver is 4.6 dB while the diversity gain of the best-sector receiver is 2.8 dB.



a)



b)

Figure 6.3: SNR of the a) maximal-ratio sectored receiver and b) non-sectored receiver as a function of position within the default configuration room.

Figure 6.4 shows the diversity gain as a function of the half-power angle of the emitter in both isotropic and mixed noise environments. Under isotropic noise only the signal has a directional behaviour and the worst-case SNR of the non-sectored, maximal-ratio and best-sector receivers is on the cell border at position (6,6). A narrower emitting beam unbalances the SNR of the sectored receiver enhancing in this way the advantages of the combining methods. This nearly compensates the higher propagation losses felt at the cell border with a narrower emitting beam. As a result, the SNRs of the sectored receivers increase with the half-power angle at a much lower rate than the SNR of the non-sectored receiver. The net effect is a decrease in the diversity gain with the half-power angle. The opposite behaviour is observed in a mixed noise environment. Now both signal and noise are directional. The worst-case SNRs coincide always with positions where the closest noise source is interposed between the receiver and the emitter. Therefore the signal and the noise come from close directions partially destroying the previous unbalancing in the SNRs of the sectored receivers. The net effect is an increase in the diversity gain with the half-power angle. As it is apparent from this discussion placing the noise sources outside the cell would result in a behaviour similar to the one observed in the isotropic noise case.

In all previous cases the worst-case SNR increases with the half-power angle. Therefore, as concluded in [3] for the case of non-sectored receivers, optical emitters should be designed with wide radiation patterns. Our study will proceed by assuming an half power angle of $hpa=60^\circ$.

Figure 6.4 shows modest gains under isotropic noise. With $hpa=60^\circ$ penalties of -0.9 dB with the maximal-ratio receiver and -2.4 dB with the best-sector receiver are incurred. This is a direct result of constraining the overall active area of the sectored receiver to be equal to the active area of the non-sectored receiver. This is exceedingly conservative since, in practice, the use of sectors with a narrow field-of-view makes it possible the use of lensed photodetectors allowing for an increase in the overall active area of sectored receivers at low cost. In addition no attempt has been made in this study to optimise the configuration of the sectored receiver for a

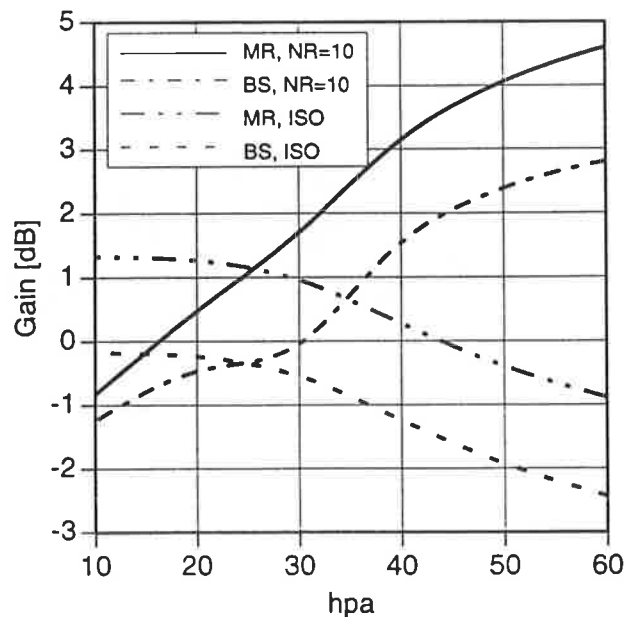


Figure 6.4: Diversity gain versus half-power angle of emitter.

particular cell range. The configuration of the sectored receiver under consideration was selected for illustrative purposes only. The optimisation of the sectored receivers will be the subject of a future contribution.

Figure 6.5 shows the diversity gain as a function of the half-power angle of the noise sources. The diversity gain increases as the half power angle of the noise sources decreases. With $NR=10$ and $hpa_n=10^\circ$ the diversity gain is 10.2 dB for the maximal-ratio receiver and 8.6 dB for the best-sector receiver. With $NR=0.5$ the gains reduce to 3.7 dB and 2.1 dB respectively. These results show the significant gains in performance of the sectored receivers in environments with directional noise sources. Also worth mentioning is that the gains of the best-sector receivers approach the gains of the maximal-ratio receivers as the half-power angle decreases. This is due to the associated concentration of the noise in fewer sectors.

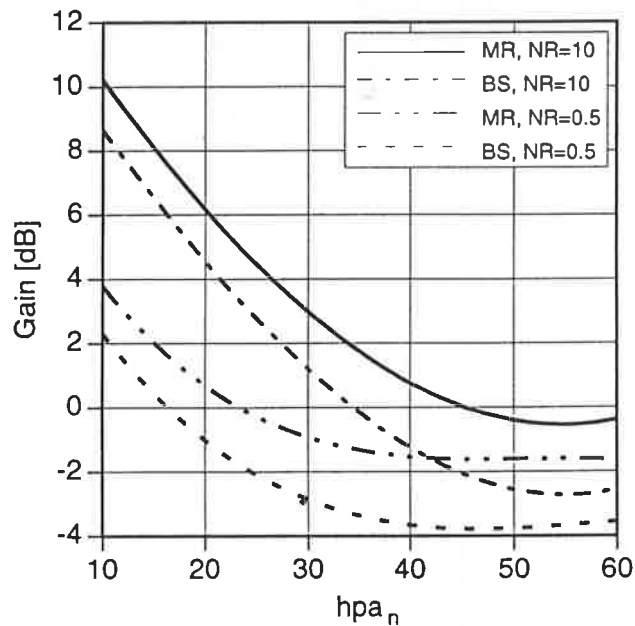


Figure 6.5: Diversity gain versus half-power angle of noise sources.

Figure 6.6 shows the diversity gain as a function of the position of the noise sources when these are changed at constant azimuth from the centre to the border of the cell. The ordinates and abscissas keep an equal absolute value while the noise sources move and we will refer to this value as p_n . In general the SNRs of the sectored receivers vary much less with the position of the noise sources than the SNRs of the non-sectored receivers. The curves show 3 different regions: near, middle and far. In the near region there is a decrease in the diversity gain. This is mainly due to an initial increase in the SNR of the non-sectored receiver due to the spreading of the noise source positions. In the middle region the diversity gain increases. Here the worst-case SNR positions of the non-sectored receiver keep close to the vertical of the noise sources causing a decrease in the SNR while moving away from the centre of the cell. In contrast the SNR of the sectored receivers increase slightly because, as the directional noise sources depart from the centre of the cell and consequently from each other, the noise distribution among the sectors becomes less uniform enhancing the advantages of the combining methods. In the far region the diversity gain decreases. As the directional noise sources depart from the cell

boundaries its relative weight decreases. In the limit, as the directional noise sources approach infinity, the noise inside the cell would tend to be purely isotropic. The curves corresponding to the maximal-ratio receivers present a discontinuity at $p_n=6$. The discontinuity takes place when changing the noise sources from being inside the cell to being outside the cell. While in the case of noise sources inside the cell there are always positions where the receiver sees the signal and the noise from similar directions, when the noise sources move to be outside the cell the receiver sees the signal power from one direction and the noise power from the opposite direction at all positions including the worst-case one. This provokes a sudden unbalancing in the SNRs of the sectored receiver enhancing the advantages of the maximal-ratio receiver. This abrupt change is not observed in the case of the best-sector receivers. Here the worst-case SNR is dominated by the sector that is pointing to the emitter and is not significantly affected by a change in the position of the noise sources. As the noise sources approach the border of the cell the gains of the maximal-ratio and best-sector receivers also approach due the prevalence of the SNR of one of the sectors. Immediately after the border of the cell the gain of the maximal-ratio receiver is 13.3 dB and the gain of the best-sector receiver is 11.7 dB. With $hpa_n=10^\circ$ the gains increase to 17.1 dB and 15.5 dB, respectively. When $hpa_n=25^\circ$ and the noise ratio drops to $NR=0.5$ the gains are 6.8 dB and 5.3 dB, respectively.

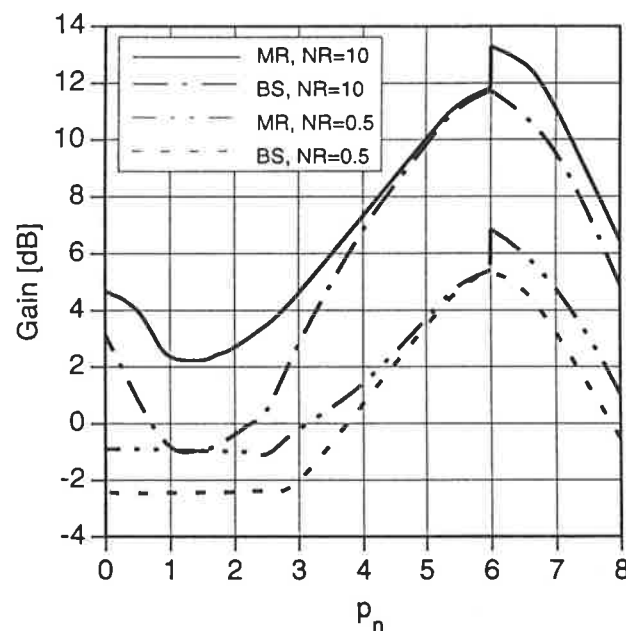


Figure 6.6: Diversity gain versus position of directional noise sources.

B. Diffuse systems

Figure 6.7 shows the diversity gain as a function of the half-power angle of the noise sources. The behaviour is similar to the diffuse case except that the gains are now higher. This is a direct consequence of having the directional noise sources inside the cell. The worst-case SNR of the best-sector receiver keeps constant since it is dominated by the isotropic noise. Given that the signal is isotropic the best-sector

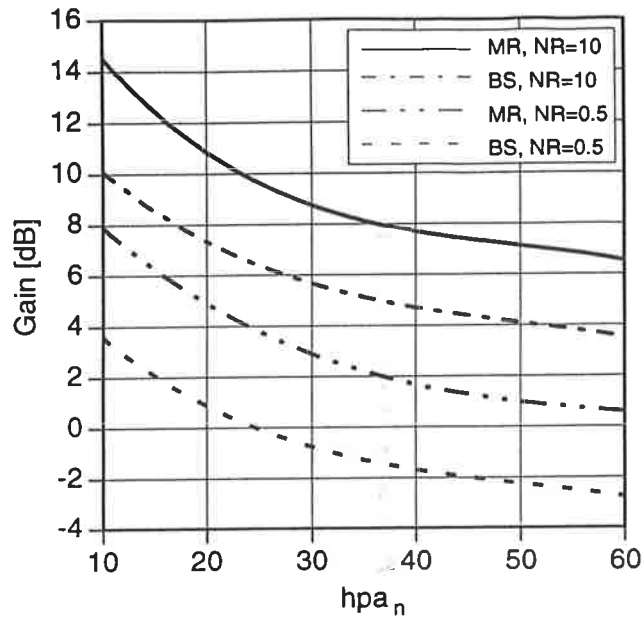


Figure 6.7: Diversity gain versus half-power angle of noise sources in diffuse system.

avoids all directional noise sources by looking at the cell boundaries. The worst-case SNR of the maximal-ratio receivers keeps also relatively constant. This is again due to the dominance of the sectors receiving only isotropic noise. Here the worst-case positions are in general near the centre where the directional noise is felt with equal intensity in the mixed noise sectors. With $NR=10$ and $hpa_n=10^\circ$ the diversity gain is 14.4 dB for the maximal-ratio receiver and 10.2 dB for the best-sector receiver. With $NR=0.5$ the gains reduce to 7.9 dB and 3.7 dB respectively.

Figure 6.8 shows the diversity gain as a function of the position of the noise sources. Again there are 3 distinct regions. Since the SNRs of the sectored receivers

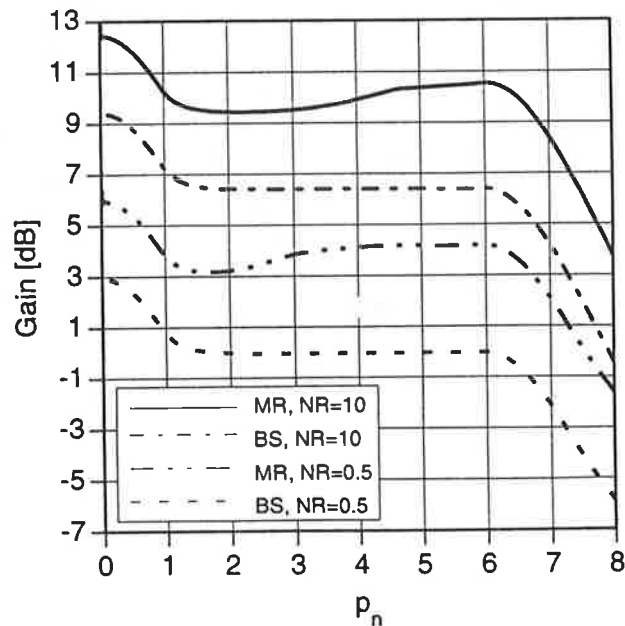


Figure 6.8: Diversity gain versus position of noise sources in diffuse system.

keep relatively constant the curves are dominated by the SNR behaviour of the non-sectored receiver. The SNR of the non-sectored receiver increases initially due to the spreading of the noise sources. When approaching the middle region the worst-case SNR position moves progressively towards the vertical of the noise sources. Thus the SNR changes from being dominated simultaneously by the 4 noise sources to being dominated by isolated noise sources. In the middle region the SNR maintains a constant level. In the far region the SNR increases again as the noise sources are getting away from the cell.

C. Diffuse versus Quasi-Diffuse systems

In order to compare the performance of diffuse and quasi-diffuse systems we show again in figure 6.9 the diversity gain as a function of the position of the directional noise sources. The diffuse system performs better for positions of the directional noise sources closer to the cell centre while the quasi-diffuse system performs better for positions of the directional noise sources closer to the cell border. We note that in the quasi-diffuse system the signal is directional while in the diffuse system the signal is isotropic. The noise conditions are the same in both systems. When the directional noise sources are closer to the centre of the cell the receiver sees the signal and the noise coming from the same direction at most of its possible locations. The percentage of such locations decreases as the directional noise sources depart from each other towards the border of the cell and after a crossover position the quasi-diffuse system will always perform better than the diffuse system. Note also that the crossover position is always lower than the cell boundary since in the case of directional noise sources positioned outside the cell the signal and the noise will come from opposite directions for all possible locations of the receiver.

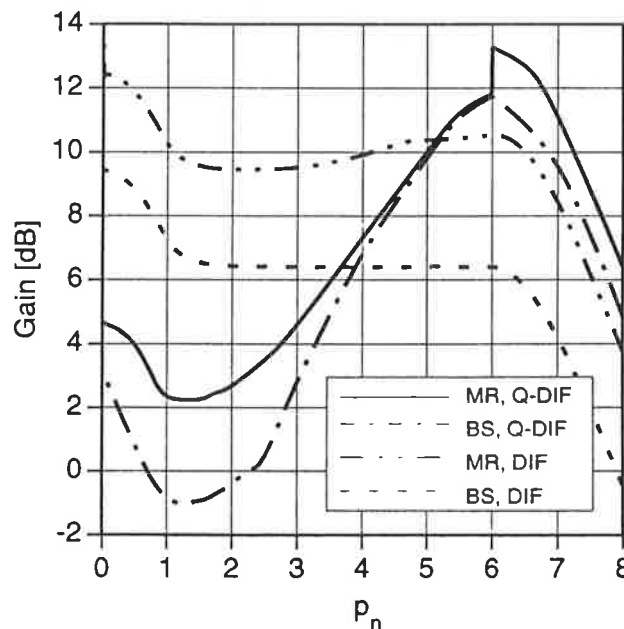


Figure 6.9: Diversity gain in diffuse and quasi-diffuse systems.

VII. Implementation Issues

The structures of the maximal-ratio and best-sector receivers are represented in figures 7.1 and 7.2 respectively. A sectored receiver requires one front-end per sector and one circuit to estimate the SNR per sector. In the case of a maximal-ratio receiver a variable gain amplifier per sector and an a summing circuit are also required whereas in the case of a best-sector receiver a selection circuit is also required.

In a packet communication system the sectored receiver settlement can be done on a per-packet basis during the initial period of the preamble. The SNR is not expected to vary significantly during the reception of a packet. The duration of settling period depends mainly on the time constants of the estimating circuits. Clearly there is a trade-off between the accuracy of the SNR estimate and the duration of the settling period. The SNR estimate can be made very simple by using a periodic signal on the preamble, e.g., a clock signal. The signal level can be estimated using the same techniques as in AGC circuits. We note that an AGC circuit is already required in non-sectored receivers due to the high-dynamic range of the optical medium. The ambient noise level can be estimated directly from the photodiode average current. However, in environments with different types of noise sources this will not suffice and the noise estimate can be derived through appropriate bandpass filtering. We may conclude that the additional complexity of sectored receivers is not significant and certainly pays-off the performance gains.

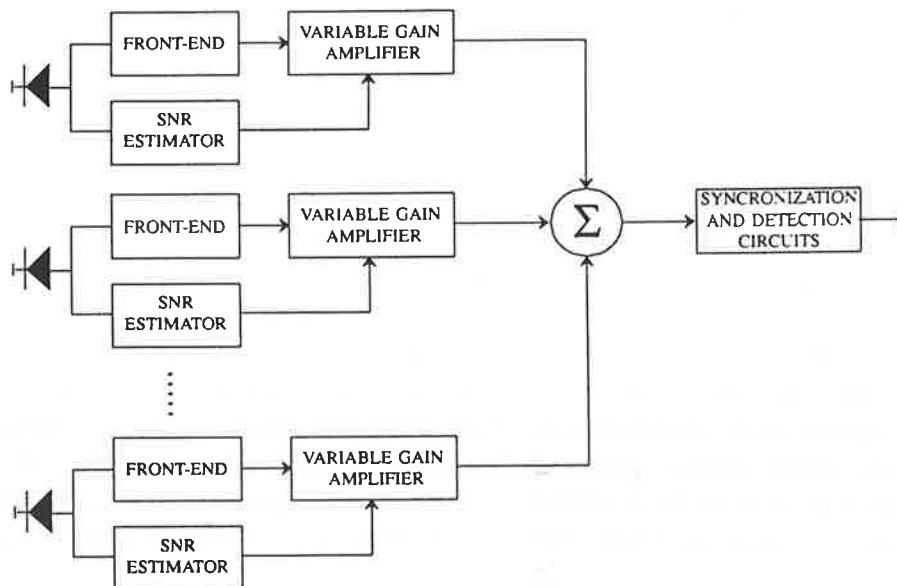


Figure 7.1: Maximal-ratio receiver structure.

When selecting a combining method the properties of the noise sources have to be considered. The sun light is stationary while the incandescent and the fluorescent lamps emit periodic light signals. The period corresponds to the mains frequency, in the case of incandescent lamps, and to the switching frequency of an electronic ballast or to the mains frequency, in the case of fluorescent lamps. The periodic interference produces correlation among the noise in each sector which degrades the performance of the maximal-ratio receiver. Noise correlation leads to an optimum sector gain of the maximal-ratio receiver that depends on the SNRs of all sectors inducing a

significant increase in the complexity of the receiver. In addition, depending on the level of noise correlation, even a maximal-ratio receiver adjusted for optimum gain could have an inferior performance in this case. In contrast the performance of the best-sector receiver is not affected by the noise correlation. Therefore, in case of systems where the interference can not be adequately filtered the best-sector receiver is always preferred. Moreover, as seen in this document, the gains of the best-sector receiver are close to those obtained with the maximal-ratio receiver.

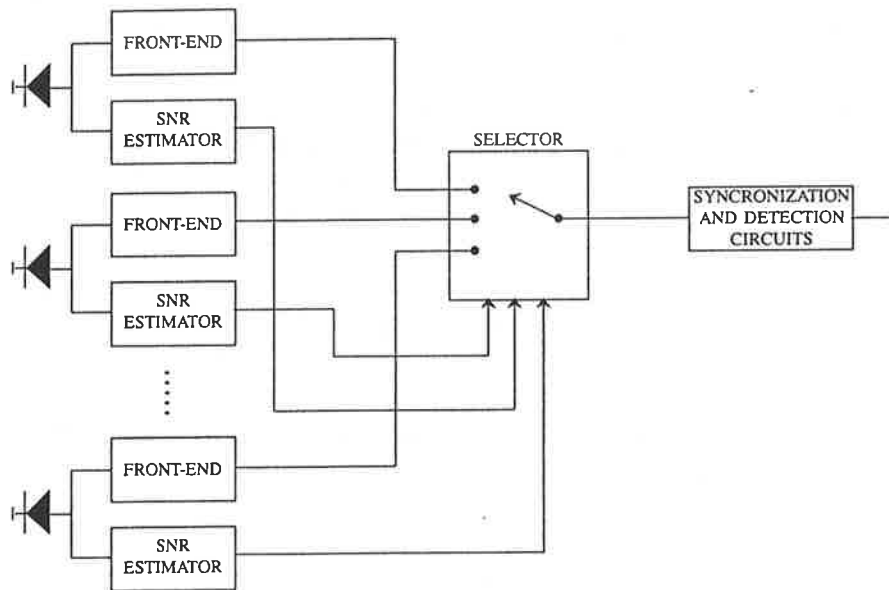


Figure 7.2: Best-sector receiver structure.

VIII. Conclusions

We conclude that the use of sectored receivers can significantly improve the performance of indoor optical wireless systems. Significant optical power gains in both diffuse and quasi-diffuse systems were demonstrated. The optical gains were seen to increase with the relative weight of the directional noise within the cell, with the sharpness of the directional noise source beam width and in environments where there are noise sources positioned outside the cell. Also the SNR of a sectored receiver was seen to be much less sensitive to the position and beam width of the noise sources than the SNR of a non-sectored receiver allowing for more universal transceiver designs. In addition a sectored receiver can be implemented with only a moderate increase in complexity.

References

- [1] - Brennan, D.G. : "Linear Diversity Combining Techniques", Proc. of the IRE, pp. 1075-1102, June 1959.
- [2] - Gfeller, F.R.; Bapst, U. : "Wireless In-House Data Communication via Diffuse Infrared Radiation", Proc. of the IEEE, Vol. 67, N° 11, November 1979.
- [3] - Lomba, C., Valadas, R., Duarte, A. : "Propagation Losses and Impulse Response of the Indoor Optical Channel: A Simulation Package", Proc. of the 1994 International Zurich Seminar on Digital Communication, March 8-11, 1994.
- [4] - Schwartz, M.; Bennett, W.R.; Stein, S. : "Communication Systems and Techniques", McGraw-Hill, 1966.
- [5] - Vogelmann, J.H.; Ryerson, J.L.; Bickelhaupt, M.H.: "Tropospheric Scatter System Using Angle Diversity", Proc. IRE, vol. 47, pp. 688-696, May 1959.